

Simultaneous multi-isotope trapping of ytterbium

T. Loftus, J. R. Bochinski, and T. W. Mossberg

Oregon Center for Optics and Department of Physics, University of Oregon, Eugene, Oregon 97403

(Received 9 May 2000; revised manuscript received 6 October 2000; published 10 April 2001)

Working with ytterbium (Yb), we demonstrate dual-isotope magneto-optic traps of extreme experimental simplicity yet containing either fermion-boson or boson-boson isotope pairs. Pairs studied include $^{171}\text{Yb}+^{172}\text{Yb}$ (a fermion-boson mixture) and $^{176}\text{Yb}+^{174}\text{Yb}$ and $^{174}\text{Yb}+^{172}\text{Yb}$ (boson-boson mixtures). Trapping is performed using the Yb $(6s^2)^1S_0-(6s6p)^1P_1$ transition, an uncooled thermal source, and bichromatic trapping beams. Static and dynamic properties of the composite cloud are conveniently probed on the spin-forbidden $(6s^2)^1S_0-(6s6p)^3P_1$ transition. A unique strategy for continuously loading these samples into magnetic traps is described.

DOI: 10.1103/PhysRevA.63.053401

PACS number(s): 32.80.Pj

Dual-isotope magneto-optic traps (DIMOTs) [1–3] provide unique gateways to studies of mixed-isotope light-assisted collisions [1,3] and, potentially, to the production of unique systems such as quantum degenerate fermionic [4] and/or fermionic-bosonic gases [2,3,5] and interpenetrating bosonic superfluids [6,7]. DIMOTs involving alkali-metal atoms have been demonstrated [1–3] but involve significant experimental complications such as the need for up to eight distinct cooling/trapping laser frequencies, isotopically enriched or artificially produced radioactive samples, and heating-induced loss of one isotope due to the trapping lasers for the other [2,3].

Ytterbium (Yb), on the other hand, provides for the realization of several distinct DIMOTs while avoiding all of these experimental complications. Comparable bosonic ($A = 168, 170, 172, 174, 176$) and fermionic ($A = 171, 173$) isotopic abundance [8] eliminates the need for isotopically enriched samples while the significant cooling power of the 398.8-nm $^1S_0-^1P_1$ transition [9–11] enables efficient trap loading directly from a thermal source [9]. Further, only two trapping-beam frequency components are required [8], a small range of frequency differences provides access to several separate isotope pairs [12], and the trapping beams for one isotope do not weaken the trap for the other [13]. Trap dynamics can be probed *nondestructively* via weak excitation of the 555.6-nm $^1S_0-^3P_1$ intercombination transition [14]. Additionally, Yb DIMOTs provide unique and to date unrealized opportunities to explore (1) cross-isotope collision dynamics in nuclear-spin-free systems, enabling quantitative comparisons with theory over a larger range of internuclear separations than is possible using alkali-metal atoms [1,3,15–18], (2) collisions between atoms with and without hyperfine structure, studies that cannot be performed with alkali-metal atoms [15,16], and ultimately (3) isotopic mixtures of quantum-degenerate fermionic and fermionic-bosonic gases. Alkaline earths, having analogous internal level structure [20], offer similar possibilities but have less favorable or varied fermionic natural abundance [21] and $^1S_0-^1P_1$ trap lifetimes that are, due to excited-state leakage, one to two orders of magnitude *shorter* than those for Yb [9,22].

In this paper, we present a realization of a $^{171}\text{Yb}+^{172}\text{Yb}$ DIMOT which comprises a fermion-boson mixture of atoms,

one with one and one without hyperfine structure. Additionally, we demonstrate DIMOTs containing $^{176}\text{Yb}+^{174}\text{Yb}$ and $^{174}\text{Yb}+^{172}\text{Yb}$ which comprise boson-boson mixtures of nuclear-spin-free atoms. Trap loading is performed using a thermal source with natural isotopic composition and bichromatic trapping beams. Adjustment of the relative power and frequency offset between the individual trapping-beam frequency components provides independent control over the constituent trap lifetimes [9] and populations. Composite cloud properties, including the relative sizes, spatial overlap, populations, and lifetimes are determined using calibrated probe and trapping-beam induced fluorescence from the 555.6 nm $^1S_0-^1P_1$ [14] and 398.8 nm $^1S_0-^1P_1$ transitions [see Fig. 1(a)]. Significantly, we obtain individual trap populations approaching the largest values previously achieved in single-isotope $^1S_0-^1P_1$ Yb MOTs [9] and peak spatial densities near the regime where intratrap collisions significantly affect trap dynamics [17,18]. Finally, we describe a unique pathway for continuously loading these samples into purely magnetic traps.

Some aspects of the apparatus have been reported elsewhere [9,14]. Other features and modifications are noted here

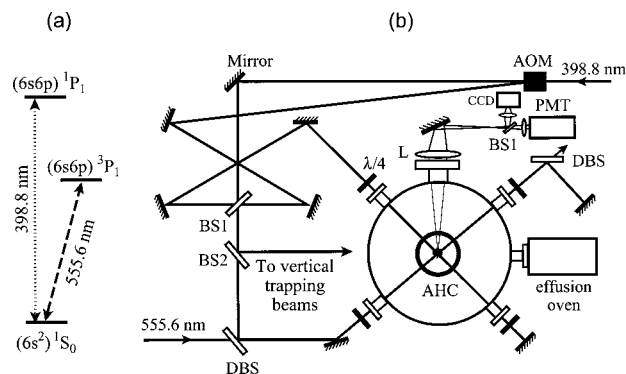


FIG. 1. (a) Partial Yb energy level diagram showing transitions relevant to the experiment. Radiative decay pathways from the 1P_1 excited state are $^1P_1 \rightarrow ^1S_0$ or $^1P_1 \rightarrow ^3D_{1,2} \rightarrow ^3P_{0,1,2}$ [9,25]. (b) Schematic diagram of the experiment in the X-Z plane. AOM, acousto-optic modulator; CCD, charge-coupled-device camera; PMT, photomultiplier tube; AHC, anti-Helmholtz magnetic field coils; L, lens; $\lambda/4$, quarter-wave plate; DBS, dichroic beamsplitter; BS1, 50/50 beamsplitter; BS2, optical flat

[see Fig. 1(b)]. The thermal Yb source comprises an effusion oven with a 2.3-mm-diameter output nozzle followed by a collimating skimmer (8 mm diameter, located 19 cm from the nozzle). A heater maintains the oven body (nozzle) at 450 °C (625 °C), resulting in a measured flux of 10^{11} atoms/sec through the observed trapping region (1 cm² cross section, 35 cm downstream from the nozzle). Fluorescence from this region is imaged onto a charge-coupled device camera (CCD, which provides ~ 75 μm resolution of trap features) and a photomultiplier tube (PMT) that is either sampled by a digital oscilloscope (500- μs overall system response time) or used in photon-counting configuration. Bandpass filters allow selective detection of either the 555.6-nm or 398.8-nm trap fluorescence. In all that follows, the axial magnetic field gradient is 60 G/cm. Vacuum levels during the experiment are less than 10^{-8} Torr.

The bichromatic trapping beams are generated by passing 80–120 mW of 398.8-nm light through an acousto-optic modulator (AOM). The resulting zeroth- (power P_0 , frequency ν_0) and upshifted first-order (power P_1 , frequency ν_1) beams are combined on a 50/50 beamsplitter (BS1), expanded to $1/e^2$ intensity diameters of 1.5 and 1 cm, respectively, and split into three pairs of trapping beams. One pair, with relative power of unity, is normal to the atomic beam and parallel to the axis of the anti-Helmholtz coils (AHC). The other two pairs, normal to the first and with relative powers of 10, intersect the atomic beam at $\pm 45^\circ$.

The weak collimated 555.6-nm probe beam is produced by a ring dye laser (long-term linewidth less than 2 MHz), combined with a trapping beam traveling normal to the AHC axis, has a $1/e^2$ intensity diameter of 5 mm, and is single passed through the atom cloud. Saturated absorption in an external Yb gas cell provides frequency markers for the Yb 1S_0 - 3P_1 resonance.

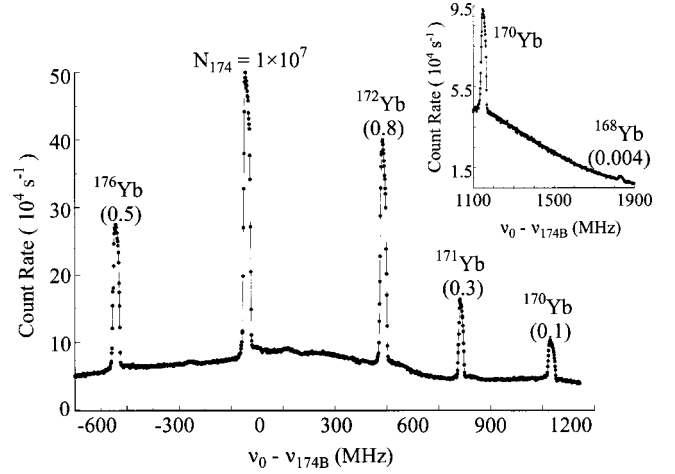


FIG. 2. 398.8-nm photocount rate collected from the trapping region when $P_0=80$ mW, $P_1=0$ (single-isotope MOT operation), and ν_0 is scanned. N_{174} is the estimated number of trapped ^{174}Yb , ν_{174B} is the ^{174}Yb 1S_0 - 1P_1 resonance frequency, and trap population ratios N_x/N_{174} are listed in parentheses. The signature for ^{173}Yb is absent presumably due to inefficient trapping caused by optical pumping in the $^1S_0(F=\frac{5}{2})$ ground state [10].

In Fig. 2, we plot the 398.8-nm photocount rate collected from the trapping region when $P_0=80$ mW, $P_1=0$ (single-isotope MOT operation), and ν_0 is scanned. ν_{174B} is the ^{174}Yb 1S_0 - 1P_1 resonance frequency, N_{174} is the estimated ^{174}Yb trap population, and population ratios N_x/N_{174} where N_x is the population for isotope x are listed in the parentheses. Note that, with the exception of ^{168}Yb (0.13% natural abundance), $N_x/N_{174} > 0.1$, and frequency shifts between several pairs are nearly equal. Consequently, for an essentially fixed value of $\delta = \nu_1 - \nu_0$, multiple isotope pairs

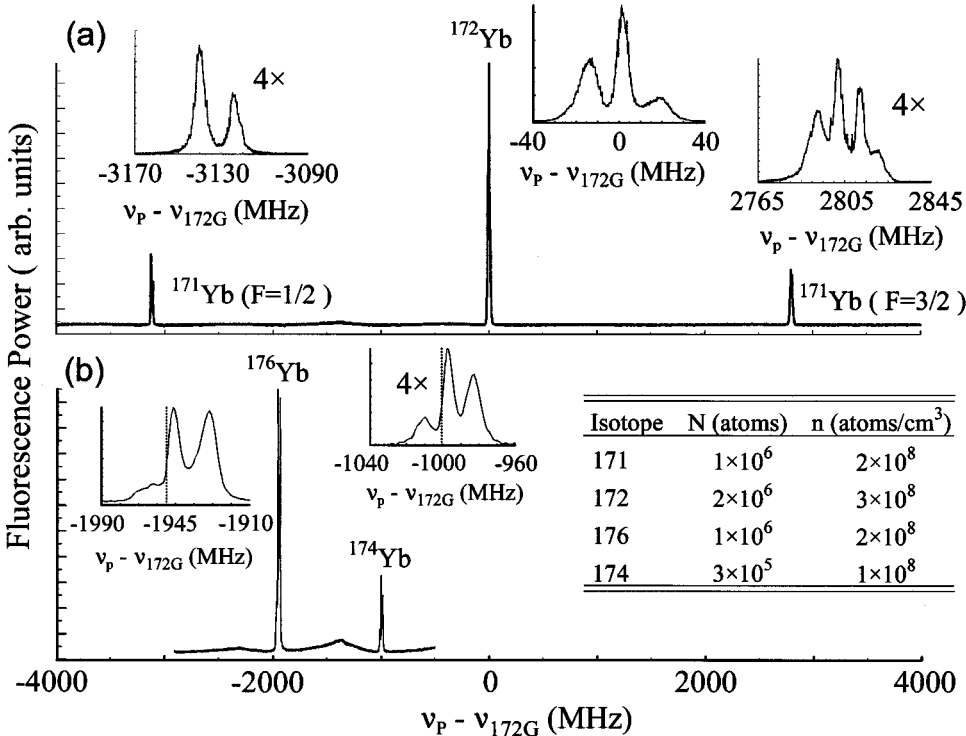


FIG. 3. 555.6-nm fluorescence spectra from (a) $^{171}\text{Yb} + ^{172}\text{Yb}$ and (b) $^{176}\text{Yb} + ^{174}\text{Yb}$ DIMOTs. ν_p (ν_{172G}) is the probe (^{172}Yb 1S_0 - 3P_1 resonance) frequency. Note that in (b) the probe polarization is orthogonal to the polarization used in (a). Dashed vertical lines in the inset to (b) give ^{176}Yb and ^{174}Yb 1S_0 - $^3P_1(m_J=0)$ resonance frequencies F is the total angular momentum for each of the two ^{171}Yb 3P_1 hyperfine excited states. Note the ^{171}Yb $^1S_0(F=\frac{1}{2})$ ground state is magnetically split only at a rate of 750 Hz/G, which is unobservable in the present context. Trap populations and peak spatial densities are listed in the table.

can be separately captured, allowing different permutations of electronic structure and quantum spin statistics to be explored in a single experiment. Moreover, N_{174} exceeds the best previous results obtained using precooled Yb atomic beams [9], indicating that efficient trap loading, essential to obtaining large DIMOT populations, is possible using a simple and compact thermal Yb source. These results have allowed us to create and study three separate Yb DIMOTs. The remainder of this work, however, will focus on mixtures of $^{171}\text{Yb}+^{172}\text{Yb}$ and $^{176}\text{Yb}+^{174}\text{Yb}$.

In Fig. 3(a), we plot the probe-induced 555.6-nm fluorescence spectra collected from the trapping region when $P_0 = 55$ mW, $P_1 = 60$ mW, δ matches the $^{172}\text{Yb}-^{171}\text{Yb}(F=\frac{3}{2})$ $^1S_0-^1P_1$ frequency shift (305 MHz [12]), and ν_0 is tuned 40 MHz below the ^{172}Yb $^1S_0-^1P_1$ resonance. In the figure, ν_P (ν_{172G}) is the probe (^{172}Yb $^1S_0-^3P_1$ resonance) frequency. The presence of three peaks, each having a unique substructure (shown in the figure insets) and separated by the $^{172}\text{Yb}-^{171}\text{Yb}(F=\frac{1}{2}, \frac{3}{2})$ frequency shifts [19] definitively demonstrates simultaneous trapping of ^{171}Yb and ^{172}Yb and illustrates the significant differences between the electronic structure of the two isotopes. Specifically, the trap magnetic field splits the ^{172}Yb fluorescence peak into three features, reflecting the simple $J=0 \rightarrow J=1$ character of the ^{172}Yb $^1S_0(J=0)-^3P_1(J=1)$ transition. In contrast, the ^{171}Yb emission features display two or four components, reflecting the trap magnetic-field splitting of the more complex $^1S_0(F=\frac{1}{2})-^3P_1(F=\frac{1}{2}, \frac{3}{2})$ transitions [14].

In Fig. 3(b), we plot the 555.6-nm fluorescence collected from the trapping region when $P_0 = 50$ mW, $P_1 = 15$ mW, δ is chosen to match the $^{176}\text{Yb}-^{174}\text{Yb}$ $^1S_0-^1P_1$ isotope shift (509 MHz [12]), and ν_0 is tuned 30 MHz below the ^{176}Yb $^1S_0-^1P_1$ resonance. Here, the presence of two fluorescence features separated by the $^{176}\text{Yb}-^{174}\text{Yb}$ $^1S_0-^3P_1$ isotope shift [19], each having three spectral components, indicates simultaneous trapping of ^{176}Yb and ^{174}Yb . We find that N_{174} is limited by the available laser power, which is small due to the low (less than 30%) diffraction efficiency exhibited by the AOM used to trap this isotope pair. Note that the frequency difference between the $^1S_0-^3P_1(m_J=0)$ resonance frequencies and the spectral location of the magnetically insensitive $^1S_0-^3P_1(m_J=0)$ fluorescence peaks [see the insets to Fig. 3(b)] reflects trapping-beam-induced Stark shifts of the 1S_0 ground state.

Along with unambiguous confirmation of simultaneous trapping, these fluorescence features provide real-time information about individual isotopes in the composite cloud. Specifically, the relative areas under the peaks (appropriately weighted to account for the ^{171}Yb hyperfine structure) give the population ratios N_{172}/N_{171} and N_{176}/N_{174} while, from the peak widths and splittings, individual cloud displacements from the magnetic-field null, S , and the radii, $\Delta S/2$, of the ^{172}Yb , ^{174}Yb , and ^{176}Yb clouds can be determined [14]. Note that the ability to observe real-time changes in relative trap populations is a powerful tool for investigating cross-isotope interactions and a useful alternative to the trap-destructive techniques employed elsewhere [2,3,16,17].

Ensuring that the two trapped isotopes occupy the same spatial volume is essential to future experiments with trapped

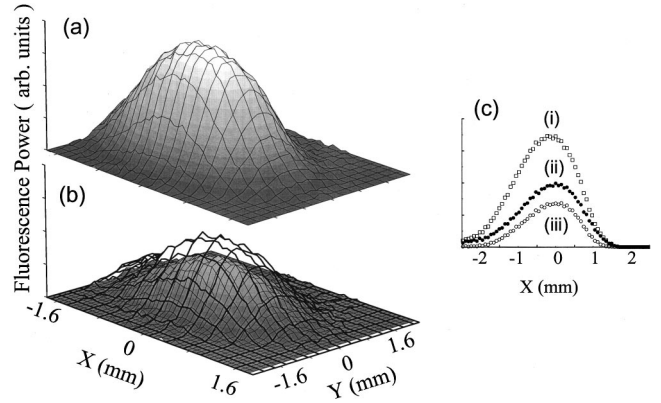


FIG. 4. 398.8-nm fluorescence as a function of position captured by the CCD under the conditions of Fig. 3(a). Y (the X - Z plane) is parallel (normal) to the AHC axis. (a) Composite $^{171}\text{Yb}+^{172}\text{Yb}$ cloud, (b) lower (upper) contour is the ^{171}Yb (^{172}Yb) fluorescence observed when the trapping beams for ^{172}Yb (^{171}Yb) are blocked. (c) Column-averaged fluorescence observed along X in (a) and (b). (i) Composite cloud; (ii) ^{172}Yb ; (iii) ^{171}Yb .

Yb isotope mixtures. In Fig. 4 we show, for the conditions of Fig. 3(a), the spatially dependent 398.8-nm fluorescence recorded by the CCD. Figure 4(a) is the fluorescence of the composite $^{171}\text{Yb}-^{172}\text{Yb}$ cloud while the lower (upper) contour in Fig. 4(b) is the ^{171}Yb (^{172}Yb) fluorescence observed when the trapping beams for ^{172}Yb (^{171}Yb) are blocked. In the figure, Y is parallel to the AHC axis. Figure 4(c) depicts the column-averaged fluorescence observed along the X coordinate in Figs. 4(a) and 4(b). Comparison of Figs. 4(a) through 4(c) shows that the ^{171}Yb and ^{172}Yb clouds are completely overlapped in the X - Y plane, while the magnetic-field-induced splitting of the 555.6-nm fluorescence reveals that cloud centers are displaced by less than 300 μm (much less than the 1-mm $1/e$ cloud radius), indicating that the individual isotope clouds occupy essentially the same spatial volume. Similar spatial overlap was observed for the $^{174}\text{Yb}+^{176}\text{Yb}$ DIMOT shown in Fig. 3(b). Using the observed cloud populations and radii, we find approximately equal peak spatial densities of $n \sim 2 \times 10^8$ atoms/cm³. For this set of parameters, we do not find conclusive evidence for cross-isotope collisions (i.e., a change in the population or loss rates [1,3] of one isotope when the other is added or removed from the composite cloud). Note, however, that the fractional contribution to total trap loss made by intratrap collisions depends critically on the electronic structure of the interacting atoms and the cloud spatial density [15–18] and the trapping laser intensity and detuning [1,3,15–18]. Future efforts will focus on increasing this contribution by optically repumping atoms shelved in the $(6s6p)^3P_{2,0}$ metastable states to increase the trap spatial density [9,17].

Observing quantum-statistical effects with cold dual or single Yb isotope samples requires significantly lower temperatures and/or higher spatial densities than observed here or in other experiments with trapped Yb. To date, ground-state magnetic trapping followed by forced rf evaporation [4,23] is the only proven strategy [24] for driving neutral atomic gases into the quantum-degenerate regime while Yb, like the alkaline-earth atoms, cannot be magnetically trapped

in the ground state. Note, however, that for the magnetic field employed in this experiment, Yb atoms in the $(6s6p)^3P_2$ ($m_J=2$) metastable state experience a magnetic potential well depth of $\sim 8 \text{ mK} \sim 10T_D$ (where $T_D=670 \mu\text{K}$ is the 1S_0 - 1P_1 Doppler-limited temperature). More importantly, for nominal Yb MOT or DIMOT populations of 10^6 - 10^7 atoms and typical trapping-beam power-limited lifetimes of 200 ms [9,10], cold atoms are *continuously* transferred to the 3P_2 ($m_J=2$) state at a rate of 10^5 - 10^6 atoms/sec [9,25]. Using a second laser ($\lambda = 648.9 \text{ nm}$) to optically pump population from the $(6s6p)^3P_0$ state to the 3P_2 ($m_J=2$) state via radiative decay from the $(6s7s)^3S_1$ state would improve this transfer efficiency by roughly an order of magnitude [25], giving, for magnetic trap lifetimes ≥ 1 sec [26], magnetic trap populations of more than 10^7 atoms. Alternatively, precooling in a 1S_0 - 3P_1 MOT [10], followed by magnetic-field switching and optical pumping to 3P_2 ($m_J=0$) via excitation of the $(6s6p)^3P_1$ - $(6s7s)^3S_1$ transition ($\lambda = 679.9 \text{ nm}$) would enable lower magnetic trap temperatures and higher spatial densities compared to the passive loading scheme described above. In either case, zero-background detection of the mag-

netically trapped atoms can be achieved using optical excitation of the $(6s6p)^3P_2$ - $(6s7s)^3S_1$ transition ($\lambda = 769.9 \text{ nm}$) followed by observation of radiative decay from $(6s7s)^3S_1$ to either $(6s6p)^3P_0$ or the $(6s6p)^3P_1$ states. Note that this entire process can be pursued with existing diode laser technology and could potentially be applied to the alkaline-earth atoms calcium and strontium [20].

In conclusion, we have presented a realization of both fermion-boson and boson-boson Yb DIMOTs, demonstrated the tremendous versatility and experimental convenience that Yb provides for these types of experiments, and described a unique pathway for magnetically trapping these cold samples. Our results are the first steps toward investigating unique types of light-assisted collision dynamics and a starting point for realizing quantum-degenerate mixtures of fermionic and bosonic Yb.

The authors wish to thank J. Bohn and D. J. Heinzen for for helpful comments and suggestions. We gratefully acknowledge financial support from the National Science Foundation under Grant No. PHY-9870223.

-
- [1] W. Süptitz *et al.*, Opt. Lett. **19**, 1571 (1994).
 [2] M. O. Mewes *et al.*, Phys. Rev. A **61**, 011403(R) (2000).
 [3] S. G. Crane, X. Zhao, W. Taylor, and D. J. Vieira, Phys. Rev. A **62**, 011402(R) (2000).
 [4] Using a mixture of ^{40}K in different internal spin states, a quantum-degenerate fermionic gas has been demonstrated. See B. DeMarco and D. Jin, Science **285**, 1703 (1999).
 [5] K. Molmer, Phys. Rev. Lett. **80**, 1804 (1998); E. Timmermans and R. Côté, *ibid.* **80**, 3419 (1998); W. Geist, L. You, and T. A. B. Kennedy, Phys. Rev. A **59**, 1500 (1999); J. P. Burke and J. L. Bohn, *ibid.* **59**, 1303 (1999).
 [6] T.-L. Ho and V. B. Shenoy, Phys. Rev. Lett. **77**, 3276 (1996); J. P. Burke, J. L. Bohn, B. D. Esry, and C. H. Greene, *ibid.* **80**, 2097 (1998).
 [7] Measurements of interpenetrating bosonic quantum fluids, using ^{87}Rb in two internal spin states, have been performed. See D. S. Hall *et al.*, Phys. Rev. Lett. **81**, 1539 (1998).
 [8] Odd (even) atomic number Yb isotopes do (do not) have 1S_0 - 1P_1 ground- and excited-state hyperfine structure and are fermions (bosons). Optical repumping of the fermionic isotopes is not required since the multiple Zeeman levels present in the 1S_0 ground state are degenerate. See Refs. [9–12], and N. Holden, in *Handbook of Chemistry and Physics*, 71st ed., edited by D. R. Lide (CRC, Boca Raton, FL, 1990), pp. 11–33.
 [9] T. Loftus, J. R. Bochinski, R. Shivitz, and T. W. Mossberg, Phys. Rev. A **61**, 051401(R) (2000).
 [10] K. Honda *et al.*, Phys. Rev. A **59**, R934 (1999); T. Kuwamoto, K. Honda, Y. Takahashi, and T. Yabuzaki, *ibid.* **60**, R745 (1999).
 [11] R. Ohmukai *et al.*, Appl. Phys. B: Lasers Opt. **64**, 547 (1997).
 [12] T. Loftus, J. R. Bochinski, and T. W. Mossberg, Phys. Rev. A **63**, 023402 (2001), and references therein.
 [13] Note that trapping transitions for isotope pairs explored here are separated by more than 10Γ where $\Gamma=28 \text{ MHz}$ is the 1S_0 - 1P_1 transition linewidth [9], and that we do not see evidence for extra loss of one isotope due to the trapping beams for the other.
 [14] T. Loftus, J. R. Bochinski, and T. W. Mossberg, Phys. Rev. A **61**, 061401(R) (2000).
 [15] A. Gallagher and D. E. Pritchard, Phys. Rev. Lett. **63**, 957 (1989); P. S. Julienne, A. M. Smith, and K. Burnett, Adv. At., Mol., Opt. Phys. **30**, 141 (1992), and references therein.
 [16] T. Walker and P. Feng, Adv. At., Mol., Opt. Phys. **34**, 125 (1994); J. Weiner, *ibid.* **35**, 45 (1995); M. G. Peters, D. Hoffmann, J. D. Tobiasson, and T. Walker, Phys. Rev. A **50**, R906 (1994).
 [17] T. P. Dinneen *et al.*, Phys. Rev. A **59**, 1216 (1999).
 [18] M. Machholm, P. S. Julienne, and K.-A. Suominen, Phys. Rev. A **59**, R4113 (1999).
 [19] W. A. van Wijngaarden and J. Li, J. Opt. Soc. Am. B **11**, 2163 (1994), and references therein.
 [20] T. Kurosu and F. Shimizu, Jpn. J. Appl. Phys., Part 1 **31**, 908 (1992); K. Sengstock *et al.*, Appl. Phys. B: Lasers Opt. Chem. **59**, 99 (1994); Th. Kisters, K. Zeiske, F. Riehle, and J. Helmcke, *ibid.* **59**, 89 (1994); C. W. Oates, F. Bondu, R. W. Fox, and L. Hollberg, Eur. Phys. J. D **7**, 449 (1999); H. Katori, T. Ido, Y. Isoya, and M. Kuwata-Gonokami, Phys. Rev. Lett. **82**, 1116 (1999).
 [21] Naturally abundant fermionic Yb isotopes are ^{171}Yb (14.3%) and ^{173}Yb (16.1%) where numbers in parentheses are the natural abundance [8]. Both have been trapped in 1S_0 - 1P_1 MOTs [9,10]. Naturally abundant alkaline-earth isotopes that can be similarly confined are ^{43}Ca (0.14%), ^{87}Sr (7%), and ^{25}Mg (10%) [8,20].
 [22] Lifetimes of ~ 900 ms were recently achieved in a Sr MOT by optically repumping atoms shelved in the 3P_2 metastable elec-

tronic state [17]. Similar lifetimes have been achieved in Yb MOTs without the use of optical repumping [9]. The Mg 1S_0 - 1P_1 trapping transition is radiatively closed and trap lifetimes of ~ 1 s have been achieved. See Ref. [20] and references therein.

[23] M. H. Anderson *et al.*, *Science* **269**, 198 (1995).

[24] Using all-optical techniques, recent experiments have nearly succeeded in generating ^{88}Sr Bose condensates. See T. Ido, Y. Isoya, and H. Katori, *Phys. Rev. A* **61**, 061403(R) (2000).

[25] S. G. Porsev, Y. G. Rakhlina, and M. G. Kozlov, *Phys. Rev. A* **60**, 2781 (1999).

[26] Assuming ambient vacuum pressures $< 10^{-8}$ Torr.